

~~MICROSTRIP DISC RESONATORS~~

Ingo Wolff and Norbert Knoppik

Translation of "Mikrostrip - Scheibenresonatoren",
Archiv für Elektronik und Übertragungstechnik,
Vol. 28, No. 3, 1974, pp. 101-108, []

(NASA-TT-F-15889) MICROSTRIP DISC
RESONATORS (Scientific Translation
Service) 29 p HC \$4.50 CSCL 09E

N74-31712

Unclas

G3/09 47764



-NATIONAL AERONAUTICS AND SPACE ADMINISTRATION-
WASHINGTON, D.C. 20546 AUGUST 1974

1. Report No.	2. Government Accession No.	3. Recipient's Catalog No.	
4. Title and Subtitle Microstrip Disc Resonators		5. Report Date August 1974	
		6. Performing Organization Code	
7. Author(s) Ingo Wolff and Norbert Knoppik		8. Performing Organization Report No.	
		10. Work Unit No.	
9. Performing Organization Name and Address SCITRAN Box 5456 Santa Barbara, CA 93108		11. Contract or Grant No. NASW-2483	
		13. Type of Report and Period Covered Translation	
12. Sponsoring Agency Name and Address National Aeronautics and Space Administration Washington, D.C. 20546		14. Sponsoring Agency Code	
15. Supplementary Notes Translation of "Mikrostrip.- Scheibenresonatoren", Archiv für Elektronik und Übertragungstechnik, Vol. 28, No. 3, 1974, pp. 101-108, A74-26581			
16. Abstract A method is presented to calculate the resonance frequencies of rectangular and circular microstrip disc resonators. The influence of the electromagnetic field distribution under the discs and the influence of the fringing field at the edge of the discs on the resonance frequencies is taken into account by defining an effective width or radius and a dynamic dielectric constant.			
17. Key Words (Selected by Author(s))		18. Distribution Statement Unclassified - Unlimited	
19. Security Classif. (of this report) Unclassified	20. Security Classif. (of this page) Unclassified	21. No. of Pages	22. Price

MICROSTRIP DISC RESONATORS

Ingo Wolff and Norbert Knoppik

1. Introduction

Resonators are spatial regions in which standing waves, / 101*
i. e., oscillations, can build up. The simplest form of a microstrip resonator can be built up using a conductive section with a length of $l = n\lambda_g/2$ ($n = 1, 2, \dots, \lambda_g$) wavelengths along the conductor) (Figure 1a), which is either open or short-circuited at the ends. Shorted line resonators are hardly ever used because it is difficult to manufacture a short circuit in strip line technology. For this reason, microstrip line resonators are used only in the form of open lines, except in special cases. The disc resonator can be considered as a degenerate line resonator of very great width. But while only one standing wave appears in the z-direction on the narrow line resonator (Figure 1a), on the disc resonator (Figure 1b) there can simultaneously be a standing wave in the x-direction, if the width w is of the order of magnitude of one half wavelength or a multiple of that. Thus, the field distribution also depends on the x-coordinate. The field distribution becomes more complex than for the narrow line resonator. The disc resonator is often used also in the circular form, as in Figure 1c. The oscillations of this resonator can be interpreted as standing radial waves which are reflected at the edge of the

* -Numbers in the margin indicate pagination in the original foreign text.

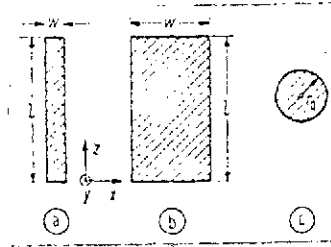


Figure 1. Plan view of the microstrip disc resonators under discussion.

resonator and at the center of the disc. In the following, we shall describe a new theory for calculation of the eigenfrequencies of individual disc resonators.

2. Calculation of the Eigenfrequencies

By the eigenfrequencies of strip line resonators, we mean the oscillation frequencies of the resonators without loading from coupled elements and without the effect of an external circuit. We must, therefore, solve the eigenvalue problem determined by the external geometric form of the resonator and the boundary conditions thus established for the electromagnetic fields, and determine the frequency at which this eigenvalue problem has a solution. The eigenvalue problems defined by the strip line resonators can be solved exactly only with difficulty. In the calculations described here, therefore, we deal with more or less accurate approximation calculations performed using an idealized resonator model.

2.1 The Circular Disc Resonator

The theory for calculation of disc resonators shall be explained by means of the circular resonator. So far, only one

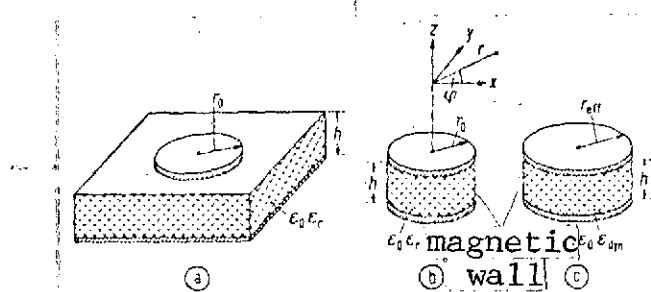


Figure 2. Circular disc resonator, (a); Resonator model according to [1], (b); and a new circular disc resonator model (c).

approximation method for calculation of the eigenfrequencies of a circular disc resonator is known from the literature. It uses a cavity model [1]. Figure 2b shows this model. It is terminated at the cover areas by two conductive circular discs, while the generated surface is formed by a magnetic wall. The diameter, r_0 , of the cover areas is equal to the diameter of the real disc on the substrate material. The height, h , of the model resonator corresponds to the height of the substrate material. The dielectric coefficient of the material which fills the model resonator is ϵ_r . If a cylindrical coordinate system is introduced according to Figure 2b, then we can find a solution for the electrical field strength of the field independent of the z -coordinate (null-type oscillations; only these occur in the frequency range of interest, due to the small substrate height, h , in the microstrip resonator) in the form

$$E_z = A J_n(kr) \begin{Bmatrix} \cos(n\varphi) \\ \sin(n\varphi) \end{Bmatrix} \quad (1)$$

Here J_n is the cylinder function of the first type (Bessel function) and k is the wave number, $k = \omega(\mu_0 \epsilon_0 \epsilon_r)^{1/2}$. Using the Maxwell equations, we can calculate the magnetic field components, from the E_z component, as

$$\begin{aligned} H_r &= \frac{n}{j\omega\mu_0 r} A J_n(kr) \begin{Bmatrix} \sin(n\varphi) \\ -\cos(n\varphi) \end{Bmatrix}, \\ H_\varphi &= \frac{k}{j\omega\mu_0} A J'_n(kr) \begin{Bmatrix} \cos(n\varphi) \\ \sin(n\varphi) \end{Bmatrix} \end{aligned} \quad (2)$$

J'_n is the derivative of the Bessel function with respect to its argument, (kr) .

The boundary conditions at the magnetic wall ($r = r_0$) require that the tangential magnetic field strength, i. e., the field component H_φ vanish for all angles φ and for the radius $r = r_0$. This means that for $r = r_0$ the derivative of the Bessel function, $J'_n(kr_0)$ must be set equal to zero. The m -th zero point of the derivative of the n -th order Bessel function occurs at the argument

$$kr_0 = 2\pi f_R r_0 / \epsilon_r c_0 = \alpha_{nm} \quad (3)$$

with f_R the eigenfrequency of the simple resonator model according to Figure 2b and c_0 the velocity of light in free space. For $m = 1$ we have

$$\alpha_{n1} = \begin{cases} 3,831 & \text{for } n=0, \\ 1,841 & \text{for } n=1, \\ 3,054 & \text{for } n=2, \\ 4,201 & \text{for } n=3. \end{cases} \quad (4)$$

Thus the E_{110} mode is the basic oscillational mode of the disc resonator, followed by the E_{210} mode, the E_{010} mode, and the E_{310} mode. Figure 3 shows the field distribution in the resonator model according to Figure 2b for the field types indicated.

If the eigenfrequencies calculated from the resonator model described, f_R , or, as is done here, the matching eigenvalues

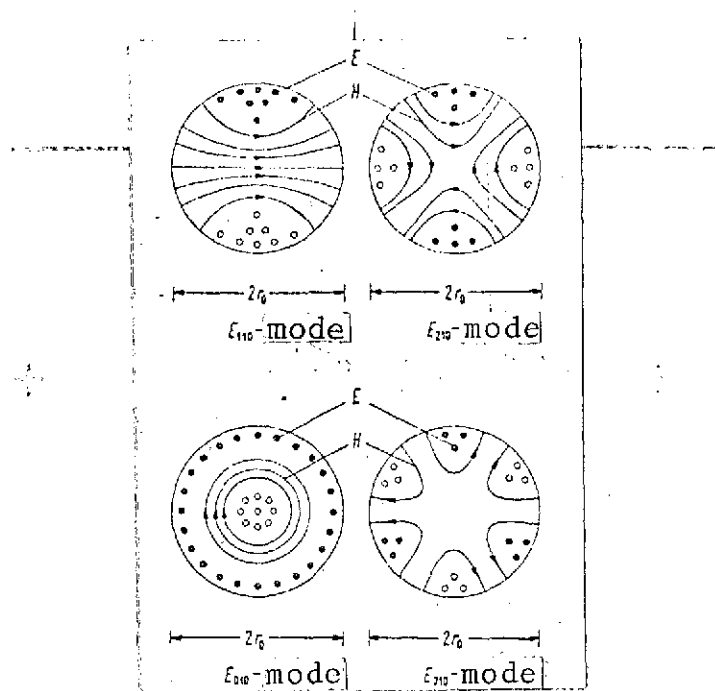


Figure 3. Field distributions in a circular disc resonator model.

according to Equation (3), are compared with the measurements (Figure 4), then deviations between the theoretically calculated and the measured frequencies appear. These deviations vary in magnitude, depending on the mode of oscillation, the resonator dimensions, and the substrate material. The measured frequencies are always lower than the calculated ones. The deviations are greatest for the eigenfrequencies of the E_{010} mode, and can amount to more than 10% for low r_0/h ratios $(r_0/h < 10)$.

In order to be able to calculate the eigenfrequencies of the resonators with better accuracy, a new model resonator is introduced (Figure 2c). An effective radius, r_{eff} , which is always greater than the actual disc radius, r_0 , takes into account the effect of the electrical and magnetic leakage fields at the edge of the resonator disc, in case the resonator is filled with

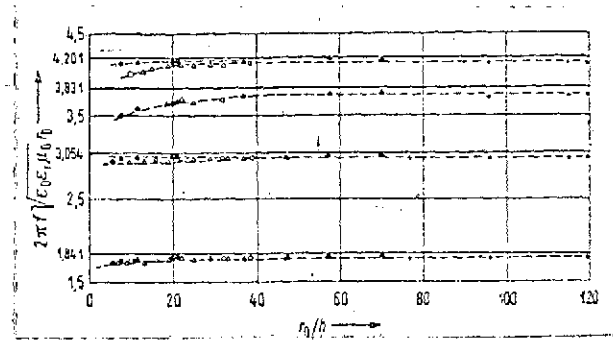


Figure 4. Comparison of the eigenvalues according to Equation (4) —, with the arguments calculated from measurements according to Equation (3) ----, plotted versus r_0/h . Substrate materials used:
 ● Al_2O_3 , $h = 0.068$ cm; ○ Polyguide, $h = 0.078$ cm;
 ▲ Polyguide, $h = 0.156$ cm; ▢ Polyguide, $h = 0.312$ cm; ▤ RT-Duroid, $h = 0.0261$ cm;
 ▴ RT-Duroid, $h = 0.0531$ cm.

air ($\epsilon_r = 1$). If the resonator has a substrate material with the dielectric coefficient ϵ_r , then the added effect of the leakage field lines, which run partially in air and partially in the dielectric, as well as the effect of the inhomogeneous field distribution in the resonator (see Figure 3) are taken into consideration by introduction of a "dynamic dielectric coefficient",
 (ϵ_{dyn}) .

/ 103

In order to define the effective radius, r_{eff} , we utilize an 1882 publication by Kirchhoff [2]. As was already shown in [3], Kirchhoff's results on calculation of the capacity of a circular disc capacitor can be used as a good approximation if the ratio of the radius to the height is greater than one ($r_0/h \gg 1$), as is always true for disc resonators. If it is assumed that the leakage field of the resonator corresponds to that of the capacitor, to a first approximation (aside from the angular dependence of the fields), then the effective radius, r_{eff} , of the disc resonator can be given approximately as [3]:

$$r_{eff} = r_0 \left\{ 1 + \frac{2h}{\pi r_0} \left[\ln \left(\frac{\pi r_0}{2h} \right) + 1,7726 \right] \right\}^{1/2} \quad (5)$$

An equivalent dielectric coefficient, ϵ_{eq} was previously given in [4]; but it can only be used to calculate the static capacity of a circular disc capacitor on substrate material ($\epsilon_r > 1$). ϵ_{eq} takes into consideration the effect of the leakage field lines running partially in air and partially in the dielectric. On the other hand, in the disc resonator we must also consider the effect of the inhomogeneous distribution of the field both under the disc and in the leakage field region on the effective dielectric coefficient (see also [5]). This dielectric coefficient is designated as ϵ_{dyn} . It is calculated by comparing the energy content of the electrical field in the resonator having a substrate material with the energy content of the field in the air-filled ($\epsilon_r = 1$) resonator. For the energy content of the principal field region, we can state that

$$W_{el} = \frac{\epsilon_0 \epsilon_r}{\delta} A^2 h \pi \left\{ \frac{r_0^2}{2} [J_n^2(kr_0) - J_{n-1}(kr_0) J_{n+1}(kr_0)] \right\} \quad (6)$$

with

$$\delta = \begin{cases} 1 & \text{for } n = 0 \\ 2 & \text{for } n \neq 0. \end{cases}$$

From this energy content we can define a dynamic principal field capacitance, $C_{o, dyn}$, by arbitrarily introducing a voltage U ,

$$U = E_z(r = r_0, \varphi = 0) h = A h J_n(kr_0) \quad (7)$$

at the edge of the disc. In this case, the E_z component of the cosine function is selected as the solution for the azimuth angle

dependence. Using Equations (6) and (7), the dynamic principal field capacitance is found to be

$$C_{0,dyn} = \frac{\epsilon_0 \epsilon_r \pi r_0^2}{\delta h} \left[1 - \frac{J_{n-1}(kr_0) J_{n+1}(kr_0)}{J_n^2(kr_0)} \right] \quad (8)$$

For $n = 0$, it follows that $C_{0,dyn} = \epsilon_0 \epsilon_r \pi r_0^2 / h$; that is, the dynamic capacitance is equal to the static capacitance of the circular disc capacitor. Furthermore, we have

$$\begin{aligned} C_{0,dyn} &= 0,3525 C_{0,stat} \quad \text{for } n = 1 \\ C_{0,dyn} &= 0,2856 C_{0,stat} \quad \text{for } n = 2 \\ C_{0,dyn} &= 0,2450 C_{0,stat} \quad \text{for } n = 3. \end{aligned}$$

If the field distribution of the resonator, which depends on the azimuth angle, φ , is also considered for the fringe field capacitance, C_e , then we can correspondingly calculate a dynamic leakage field capacitance, $C_{e,dyn}$:

$$C_{e,dyn} = \frac{1}{2\pi} \int_0^{2\pi} C_{e,stat} \cos^2(n\varphi) d\varphi = \frac{1}{\delta} C_{e,stat} \quad (10)$$

with δ according to Equation (6). The dynamic dielectric coefficient, ϵ_{dyn} , is defined from the dynamic total capacitance

$$C_{dyn} = C_{0,dyn} + C_{e,dyn} \quad (11)$$

by taking the quotient of the dynamic total capacitance of the resonator on carrier material and the dynamic total capacitance of the resonator with an air filling:

$$\epsilon_{dyn} = \frac{C_{dyn}(\epsilon = \epsilon_0 \epsilon_r)}{C_{dyn}(\epsilon = \epsilon_0)} \quad (12)$$

The dynamic dielectric coefficient, ϵ_{dyn} , is a function of the geometric dimensions of the resonator, the dielectric coefficient, ϵ_r , and of the mode of oscillation under investigation. Considering the effective radius, r_{eff} , according to Equation (5) and the dynamic dielectric coefficient, ϵ_{dyn} , we can calculate the eigenfrequencies, f_0 , of the resonator from the relation [see Equation (3)]

$$2\pi f_0 \cdot r_{eff} \sqrt{\epsilon_{dyn}/\epsilon_0} = \alpha_{nm} \quad (13)$$

with α_{nm} for $m = 1$ according to Equation (4).

As it is well known (e. g., [6]) that the electromagnetic field concentrates in the region of the dielectric with rising frequency in the presence of a dielectric-air boundary, and because a corresponding effect must also occur with the microstrip disc, the dynamic dielectric coefficient, ϵ_{dyn} , is also considered to be frequency-dependent. As was found empirically, the dynamic dielectric coefficient, ϵ_{dyn} , depends linearly on the frequency. The proportionality factor depends on the diameter of the disc and on the dielectric coefficient, ϵ_r (see also [7]).

Figure 5 shows the dynamic dielectric coefficient of the circular disc resonator calculated as a function of r_0/h for $\epsilon_r = 10.4$ and for a height, $h = 0.068$ cm, of substrate material. Different magnitudes of dynamic dielectric coefficients appear for the various modes of oscillation. In particular, the dynamic dielectric coefficient for the E_{010} mode of oscillation is considerably greater than that for the other field modes. With diminishing values of r_0/h , ϵ_{dyn} first becomes monotonically smaller. For very small values of r_0 , the eigenfrequencies of the resonators become very large. This, considering the frequency-dependence of the dynamic dielectric coefficient, leads to a renewed increase of ϵ_{dyn} .

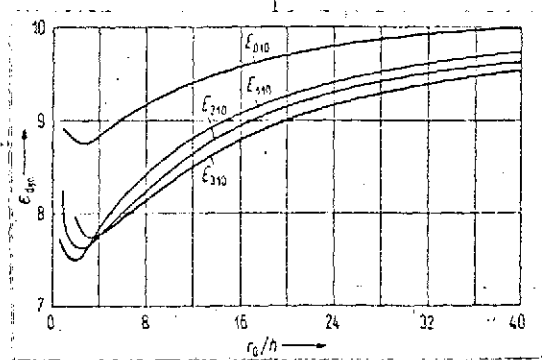


Figure 5. Calculated dynamic dielectric coefficient for the circular disc resonator as a function of r_0/h for various types of oscillation (Al_2O_3 material); $\epsilon_r = 10.4$, $h = 0.068$ cm.

The percentage deviation, Δ/f , of the eigenfrequencies f_0 and f_R according to the two resonator models (Figure 2b and 2c), $\Delta/f = [f_0 - f_R]/f_0$, referred to f_0 , is plotted in Figure 6. The deviations are considerable, especially for the E_{010} mode. For small values of r_0/h ($r_0/h \approx 10$) they are of the magnitude of 8%. The deviation Δ/f is always negative for the resonators under consideration. That is, the eigenfrequencies of the resonator models according to Figure 2c are smaller than those of the resonator model according to Figure 2b.

If the measured resonance frequencies of resonators on different substrate materials (Al_2O_3 , $\epsilon_r = 10.4$; Polyguide, $\epsilon_r = 2.315$; Duroid, $\epsilon_r = 2.23$) having different heights, h , are compared with the eigenfrequencies calculated from Equation (13), a maximum deviation of 1% is found. As Figure 7 shows, this applies over the whole region of r_0/h ratios investigated from $r_0/h = 4$ to $r_0/h = 120$.

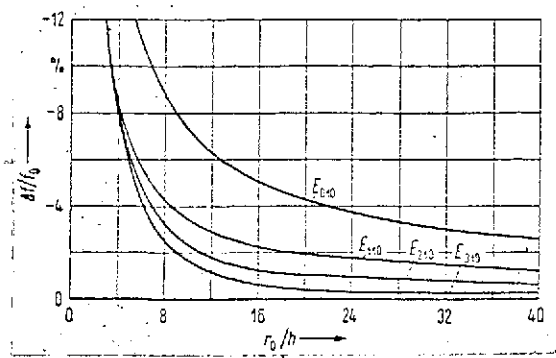


Figure 6. Calculated deviation of the eigenfrequency f_R according to Equation (3) from the eigenfrequency f_0 according to Equation (13): $\Delta f = |f_0 - f_R|$ referred to f_0 for various types of oscillation in a circular disc resonator on Al_2O_3 material; $\epsilon_r = 10.4$, $h = 0.068$ cm.

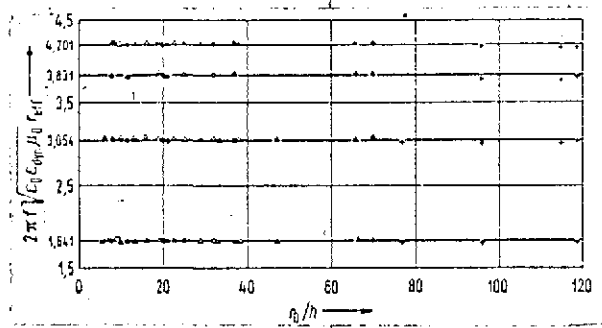


Figure 7. Comparison of the eigenvalues for the eigenfrequencies f_0 according to Equation (13) with measurements. See Figure 4 for substrate materials.

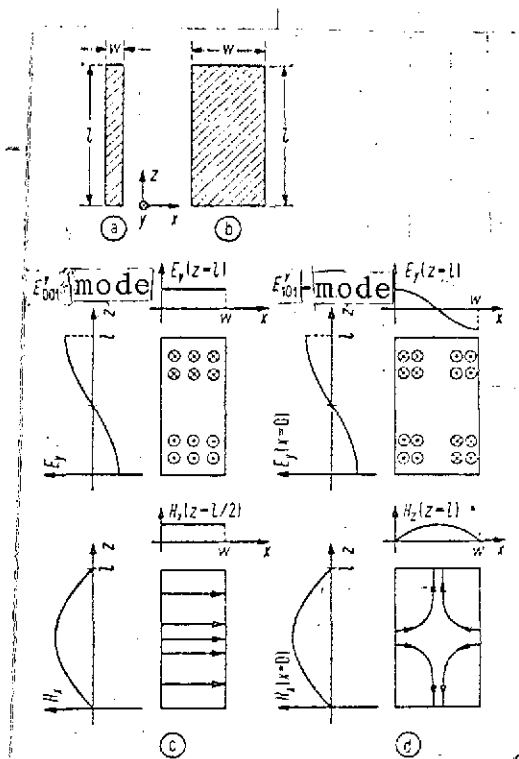


Figure 8. Rectangular sheet resonators: (a) line resonator type; (b) sheet resonator type, with a schematic representation of the field for one line resonance; (c) (E_{001}^x type) and one sheet resonance; (d) (E_{101}^y type)

2.2 The Rectangular Sheet Resonator

In order to calculate the eigenfrequencies of the rectangular sheet resonator (Figure 1a and 1b), we must differentiate between line resonances and sheet resonances. While the line resonances have a field dependence on only one coordinate (e. g., on the coordinate z , Figure 8a), the sheet resonances are defined so that their fields always depend on two coordinates (x and z , Figure 1 and Figure 8). Both of these groups of oscillation modes are treated in the following.

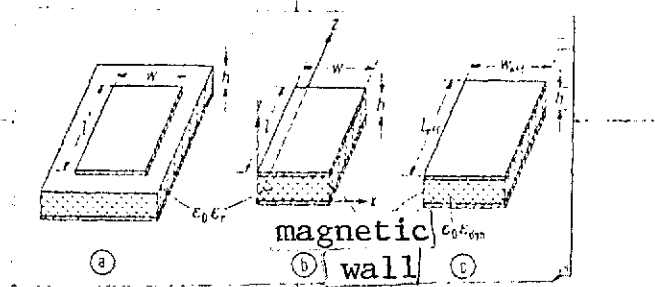


Figure 9. Rectangular sheet resonator (a); simple cavity model (b); and a new cavity model (c).

2.2.1 The sheet resonances.

We can state a simple theory for calculating the eigenfrequencies of the sheet resonances using a cavity model, as for the circular disc resonators. This first model, again, is built up so that the electromagnetic field appears only under the sheet. That is, the leakage field of the sheet resonator at the edges of the sheet is neglected; the resonator is terminated at the sides by an electrical open circuit (a magnetic wall) (Figure 9b). As no tangential magnetic field strength can exist in the magnetic wall, and because only the oscillation modes independent of the height coordinate (E^Y modes, see coordinate system in Figures 1 and 8) can be excited in the resonator for a very small height, h , of the substrate material, the eigenfrequencies of this resonator model can be calculated by the relation:

$$f_R = \frac{c_0}{2\sqrt{\epsilon_r}} \sqrt{\left(\frac{m\pi}{W}\right)^2 + \left(\frac{n\pi}{L}\right)^2}, \quad m, n = 0, 1, 2, \dots \quad (14) \quad \underline{/105}$$

Due to the fact that the entire leakage field of the resonator is neglected in the derivation of Equation (14), it is generally relatively inaccurate (see also the discussion at the end of this section).

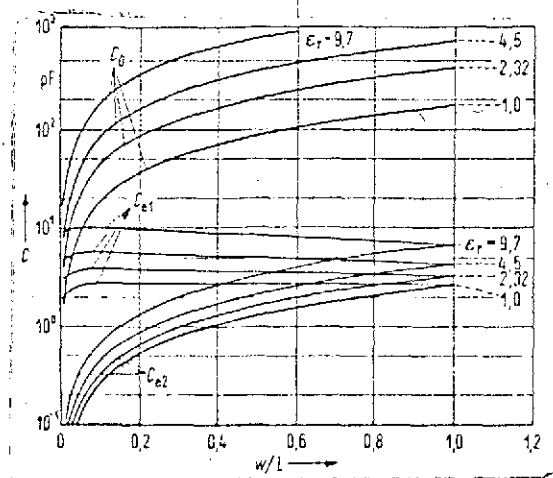


Figure 10. Static principal field capacities (C_0) and fringing field capacities for one edge with the length l (C_{e1}) or with the length w (C_{e2}) for a rectangular microstrip sheet capacitor; parameter, dielectric coefficient, ϵ_r ; $l = 10$ cm, $h = 0.05$ cm.

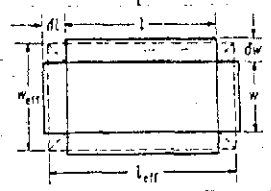


Figure 11. On the calculation of w_{eff} and l_{eff} .

In order to discuss the effect of the leakage field at the lateral edges, we first show in Figure 10 the static leakage capacitances C_{e1} at the sides of the length l , and C_{e2} at the sides of the length w for a rectangular sheet capacitor, as compared to the static capacitance C_0 of the sheet capacitor without the leakage field. As can be found from the theory of the rectangular sheet capacitor (see Equation (6) from [4]), the effect of the leakage capacitances can be understood in analogy with the discussions for the circular disc capacitor, in that the total capacitance is calculated as for the capacitance of an ideal plate capacitor with equivalent width and equivalent length, filled with a material having the dielectric coefficient ϵ_{eq} .

As for the circular disc capacitor, an appropriate model is also selected to calculate the eigenfrequencies of the rectangular resonator. The model resonator has the dimensions l_{eff} and w_{eff} , the height h and a dielectric coefficient ϵ_{dyn} (Figure 9c). It is terminated by conductive surfaces at the cover planes and by magnetic walls at the side surfaces. The effective edge lengths are first calculated separately, as for the effective width of an air-filled microstrip line [8]. In addition, an edge correction is made so that the sheet area A of the rectangular model resonator ($A = w_{eff}l_{eff}$) is identical with the area obtained by increasing the actual edges (edge lengths l and w) by the lengths δl and δw for the leakage field region according to [8] (heavily bordered area in Figure 11).

As for the circular disc resonator, a dynamic dielectric coefficient is also defined for the rectangular sheet resonator. It describes both the effect of the leakage field in the air and dielectric regions and the influence of the inhomogeneous field distribution on the effective dielectric coefficient. If it is assumed that the electric field strength of the principal field

region under the sheet is described by

$$E_y = A \cos\left(\frac{m\pi}{w}x\right) \cos\left(\frac{n\pi}{l}z\right) \quad (15)$$

and that this region is filled with a dielectric having the dielectric coefficient ϵ_r , then for the energy content of the electrical field in this region we get

$$\begin{aligned} W_{el} &= \frac{1}{2} A^2 h \epsilon_0 \epsilon_r \int_0^l \int_0^w \cos^2\left(\frac{m\pi}{w}x\right) \cos^2\left(\frac{n\pi}{l}z\right) dx dz \\ &= \frac{1}{2} A^2 h \epsilon_0 \epsilon_r \frac{wl}{\delta \eta} \end{aligned} \quad (16)$$

with $\eta = \begin{cases} 1 & \text{for } m = 0 \\ 2 & \text{for } m \neq 0 \end{cases}, \quad \delta = \begin{cases} 1 & \text{for } n = 0 \\ 2 & \text{for } n \neq 0 \end{cases}.$

Again, a voltage U is arbitrarily defined as the product of E_y and h at the location $x = 0$ and $z = 0$:

$$U = E_y(x=0, z=0)h = Ah \quad (17)$$

and the dynamic principal field capacitance, $C_{0, \text{dyn}}$, is calculated with it:

$$C_{0, \text{dyn}} = \frac{2 W_{el}}{U^2} = \frac{\epsilon_0 \epsilon_r lw}{h \eta \delta} = \frac{C_{0, \text{stat}}}{\eta \delta} \quad (18)$$

For a homogeneous field distribution of the electrical field strength, $m = 0$ and $n = 0$, so that $\eta = \delta = 1$ and $C_{0, \text{dyn}} = C_{0, \text{stat}}$. By averaging over the cosine-formed field distribution, we obtain the dynamic leakage field capacitance at the edges as:

$$\begin{aligned} C_{e1, \text{dyn}} &= \frac{C_{e1, \text{stat}}}{l} \int_0^l \cos^2\left(\frac{n\pi}{l}z\right) dz = C_{e1, \text{stat}} \frac{1}{\delta} \\ C_{e2, \text{dyn}} &= \frac{C_{e2, \text{stat}}}{w} \int_0^w \cos^2\left(\frac{m\pi}{w}x\right) dx = C_{e2, \text{stat}} \frac{1}{\eta} \end{aligned} \quad (19)$$

Now ϵ_{dyn} is calculated according to Equation (12) from the dynamic total capacitance:

$$\bar{C}_{dyn} = C_{0,dyn} + 2C_{e1,dyn} + 2C_{e2,dyn} \quad (20)$$

The eigenfrequency of the H_{m0n}^y mode of the rectangular sheet resonator is calculated from

$$f_0 = \frac{c_0}{2\sqrt{\epsilon_{dyn}}} \sqrt{\left(\frac{m}{w_{eff}}\right)^2 + \left(\frac{n}{l_{eff}}\right)^2} \quad (21)$$

using the cavity model defined according to Figure 9c.

Figure 12 shows how the eigenfrequencies calculated according to Equation (21) differ from the eigenfrequencies calculated according to Equation (14) for the H_{101}^y mode. In this case, $\Delta f = f_0 - f_R$. The deviation Δf of the eigenfrequencies of the model according to Figure 9c and Figure 9b is always negative for $\epsilon_r = 2.315$ (material Polyguide, Figure 12a). That is, the eigenfrequency of the newly introduced model according to Figure 9c is always lower than that of the simple resonator model according to Figure 9b. If, on the other hand, the difference Δf is plotted for a material with greater dielectric coefficient (Al_2O_3 , $\epsilon_r = 10.4$, Figure 12b), then Δf first becomes negative for small values of w (at constant value of l). That is, the eigenfrequencies calculated from Equation (21) are lower than those from Equation (14). For a certain ratio of w/l , Δf becomes equal to zero. For larger ratios of w/l , Δf becomes positive. That is, f_0 is greater than f_R . According to Equation (21), f_0 is inversely proportional to $(\epsilon_{dyn})^{1/2}$ and, furthermore, independent of w_{eff} and l_{eff} . For low ratios of w/l , the dielectric coefficient ϵ_{dyn} becomes much smaller than ϵ_r (at constant length, l); but it always passes through a limited range of values. In contrast,

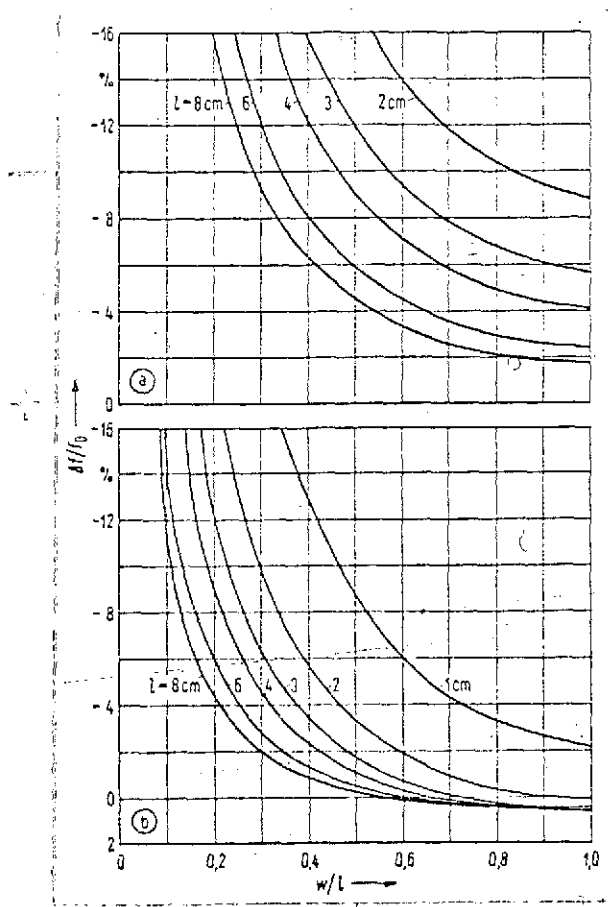


Figure 12. Calculated deviation of the eigenfrequency f_R according to Equation (14) from the eigenfrequency f_0 according to Equation (21):

$\Delta f/f_0 = (f_R - f_0)/f_0$ referred to f_0 for the E_{101} type of a rectangular sheet resonator. Parameter: resonance length l ; (a) on Polyguide material ($\epsilon_r = 2.315$, $h = 0.156$ cm); (b) on Al_2O_3 material ($\epsilon_r = 10.4$, $h = 0.068$ cm).

the root expression for $\omega \rightarrow 0$ approaches infinity in Equation (14), while the root expression in Equation (21) at this boundary transition is always very much smaller than that from Equation (14), because w_{eff} is very much greater than w for small values of w . It follows from this that there is a very large deviation, Δf , always negative, for small values of w . For large values of w , in contrast, w_{eff} is approximately equal to w , so that effect of the dielectric coefficient $\epsilon_{\text{dyn}} (\epsilon_{\text{dyn}} < \epsilon_r)$ on the eigenfrequencies prevails and f_0 can become larger than f_R . This is particularly the case for large values of ϵ_r , because in this case the relative deviation of ϵ_{dyn} from ϵ_r becomes large. For the measurements, see Section 2.2.3.

2.2.2 The line resonances

As mentioned previously, those oscillation modes with fields which depend only on one coordinate, x or z , (Figure 8 a, c) are designated as line resonances. These oscillation modes are designated as E_{m00}^x or E_{00n}^z modes. Their field distributions correspond to those of the quasi-TEM modes on the microstrip lines. Resonators in which these types are excited can be treated, in a first approximation, as open-ended line resonators, the eigenfrequencies of which are derived from the condition that the line length, l (E_{00n}^z modes) or the line width, w (E_{m00}^x modes) is a multiple of the half-wave length:

$$f_L = n \frac{c_0}{2l\sqrt{\epsilon_{\text{eff}}(w)}} \text{ OR } f_L = m \frac{c_0}{2w\sqrt{\epsilon_{\text{eff}}(l)}}, \quad (22)$$

where ϵ_{eff} is the effective real static dielectric coefficient according to Wheeler [8] or Schneider [9] for a microstrip line of width w or l , respectively.

Equation (22) does not consider the effect of the leakage field at the end of the line, nor the frequency dependence of the

effective dielectric coefficient. In order to learn the effect of the leakage field, the leakage capacitances C_{e1} and C_{e2} at the ends of the lines were calculated by the method described in [4] (e. g., for the E_{00n}^y mode the leakage capacitance C_{e2}):

$$C_{e2} = \frac{1}{2} \left(\frac{1}{Z_{D2} v_{ph2}} - \frac{\epsilon_0 \epsilon_r l}{h} \right) w. \quad (23)$$

Here v_{ph2} is the phase velocity and Z_{D2} the characteristic impedance for a microstrip line with the width l on a carrier material with the dielectric coefficient ϵ_r .

The end capacitances, C_{e2} , are recalculated in short open-ended line segments having the characteristic impedance of the line to which they are connected. These line segments always have the length Δl . This length can be calculated from the characteristic impedance of the microstrip line of width w [8] /107

$$Z_{D1} = \sqrt{\frac{\mu_0}{\epsilon_0}} \frac{h}{\sqrt{\epsilon_{eff}(w)} w_{eq}} \quad (24)$$

and from the end capacitances C_{e2} according to Equation (23):

$$\Delta l = \frac{w}{2 w_{eq} \epsilon_{dyn}(w)} (\epsilon_{eff}(l) l_{eq} - \epsilon_r l). \quad (25)$$

A corresponding relation can be derived for Δl (E_{n00}^y modes) by exchanging w and l in Equation (25). In Equation (24) and Equation (25), $\epsilon_{eff}(w)$ and $\epsilon_{eff}(l)$ are the static dielectric coefficients for the lines of corresponding width. $\epsilon_{dyn}(w)$ is the dynamic dielectric coefficient already defined in Section 2.2.1, considering the leakage capacitance, C_{e1} , at the edges of the resonator with the length l ($C_{e2} = 0$). w_{eq} is the effective strip conductor width according to Wheeler [8]. With this assumption, $\epsilon_{dyn}(w)$ is equal to the static effective dielectric coefficient $\epsilon_{eff}(w)$ for the frequency $f = 0$ [8]. For frequencies greater than zero, ϵ_{dyn} also considers the frequency-dependent properties of

the microstrip line. If ϵ_{dyn} is replaced in Equation (25) by the value $\epsilon_{\text{eff}}(w)$, we can use it in order to calculate in a simple manner the effect of the leakage field at the ends of the line resonator, as an approximation.

The eigenfrequencies of the line resonances are calculated as

$$f_0 = n \frac{c_0}{2L\sqrt{\epsilon_{\text{dyn}}(w)}} \quad \text{for } E_{00n}^y \text{ modes}$$

and

$$f_0 = m \frac{c_0}{2W\sqrt{\epsilon_{\text{dyn}}(l)}} \quad \text{for } E_{m00}^y \text{ modes} \quad (26)$$

Here L and W are the effective active lengths of the resonators for the line resonances:

$$W = w + 2\Delta w, \quad L = l + 2\Delta l. \quad (27)$$

The change in length, $2\Delta l$ according to Equation (25) is plotted in Figure 13 for line resonators of different lengths on Polyguide material. For large line widths ($w/l > 0.3$) and large line lengths l ($l > 2 \text{ cm}$), Δl can, as a first approximation, be considered independent of w/l , while Δl changes strongly for small values of w/l . Figure 14 shows the percentage relative deviation of the eigenfrequency f_0 [Equation (26)] from the eigenfrequency f_L [Equation (22)]. This deviation is smaller than zero for all values of w/l . That is, the frequency f_0 is always below f_L . As can be seen from Figure 14, the error in the calculation of the eigenfrequencies is some 10%, especially for short resonators.

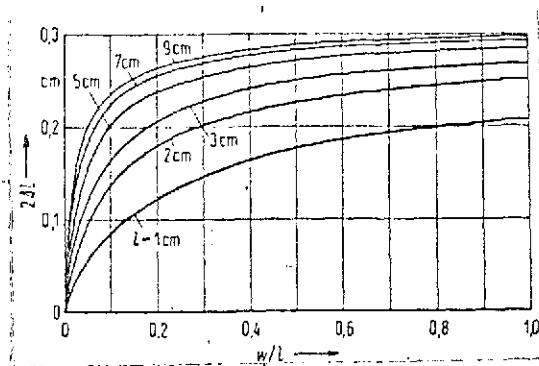


Figure 13. Change in length $2\Delta l$ for a line resonator with consideration of the scattered fields at the ends of the resonator, versus w/l ; parameter, resonator length l ; E_{001} type, $\epsilon_r = 2.315$, $h = 0.156$ cm.

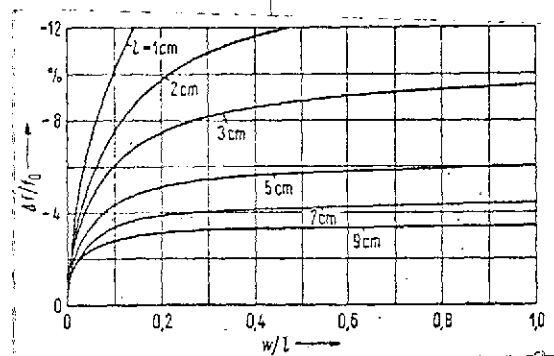


Figure 14. Calculated deviation of the eigenfrequencies f_L according to Equation (22) and f_0 according to Equation (26): $\Delta f = f_0 - f_L$ referred to f_0 for the E_{001} line type of a rectangular sheet resonator on Polyguide material; parameter, resonator length l ; $\epsilon_r = 2.315$, $h = 0.156$ cm.

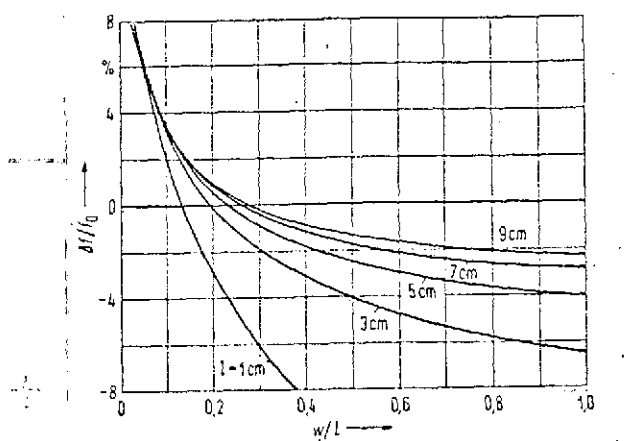


Figure 15. Calculated deviation of the eigenfrequency f_R according to Equation (14) and f_0 according to Equation (26): $\Delta f = f_0 - f_R$ referred to f_0 for the E_{001} line type of a rectangular sheet resonator on Polyguide material; parameter, resonator length, l ; $\epsilon_r = 2.315$, $h = 0.156$ cm.

In Figure 15, the eigenfrequencies f_0 according to Equation (26) are compared with the eigenfrequencies f_R according to Equation (14) for $m = 0$. In contrast to Figure 12b, the deviation, Δf ($\Delta f = f_0 - f_R$) becomes positive for low values of w/l (at constant value of l) and negative for large values of w/l . The reason for this is that the eigenfrequency f_R , according to Equation (14), is independent of w for $m = 0$. The eigenfrequency f_0 , from Equation (26), however, becomes larger for diminishing values of w , as in this case both L and ϵ_{dyn} become smaller. The value of Δf becomes zero for conductor widths w , at which the relation [see Equation (14) and Equation (26)]

$$\sqrt{\epsilon_r} l = \sqrt{\epsilon_{dyn}} L \quad (28)$$

is fulfilled. This means that in this case the simple cavity model of Figure 9b gives a good approximation for the eigenfrequencies of the line resonator.

2.2.3 Measurements

Figure 16 shows a comparison between the measured resonance frequencies, f_m , and the calculated eigenfrequencies of sheet and line resonators on various substrate materials. The "eigenvalues" assigned to the measured frequencies, f_m :

$$\begin{aligned} p &= 2f_m \sqrt{\epsilon_0 \epsilon_{dyn}(w)} \mu_0 L = n \\ \text{or} \quad p &= 2f_m \sqrt{\epsilon_0 \epsilon_{dyn}(l)} \mu_0 W = m \end{aligned} \quad (29)$$

are plotted for the line resonances, and

$$p = \frac{2f_m \sqrt{\epsilon_0 \epsilon_{dyn} \mu_0}}{\sqrt{\left(\frac{1}{n w_{eff}}\right)^2 + \left(\frac{1}{m l_{eff}}\right)^2}} = mn \quad (30)$$

for the sheet resonances. This representation makes possible a comparison of the measured and calculated frequencies of resonators with different dimensions on different substrate materials in a single diagram. As follows from Equations (29) and (30), the eigenvalues for the line resonances with $m = n$ and the eigenvalues of the sheet resonances with the same value of mn do not differ in Figure 16. The deviations of the measured resonance frequencies of the line resonances from the values calculated according to Equation (26) are clearly less than 1%. On the other hand, the deviations of the measured and calculated sheet resonance frequencies are in the order of magnitude of 1% to 2%. As extensive technological investigations show, these deviations are due to the fact that the sheet resonances are in part difficult to excite and for that reason the resonators must be more closely coupled to the external measuring system.

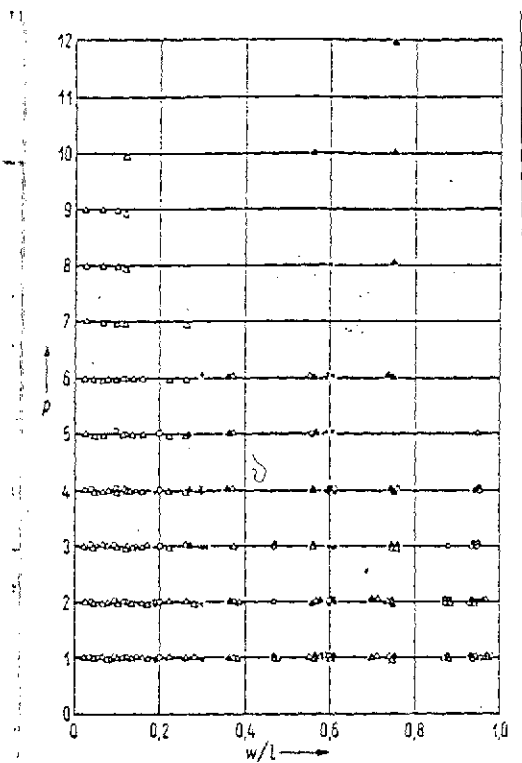


Figure 16. Comparison of the "eigenvalues", p , assigned to the measured frequencies [Equations (29) and (30)] with the eigenvalues determined from Equation (21) (sheet resonances) or from Equation (26) (line resonances), plotted versus w/l . Measured points: Δ line type (LT), \triangle disc type (ST) on Polyguide, $h = 0.156$ cm; $+$ LT, \times ST on RT-Duroid, $h = 0.0261$ cm; \square LT, \circ ST on RT-Duroid, $h = 0.0531$ cm; \oplus LT, \odot ST on Al_2O_3 , $h = 0.068$ cm. The measurements are plotted for resonators of different lengths (frequency range 1 GHz to 12 GHz).

3. Conclusions

A method for calculating the eigenfrequencies of circular and rectangular microstrip disc resonators is described. Line resonators are treated as a special case of the rectangular sheet resonator. A model resonator with effective edge lengths, filled with a material having the dynamic dielectric coefficient ϵ_{eff} , takes into consideration both the effect of the leakage field on the effective dimensions and the influence of the leakage field and the inhomogeneous field distribution of the leakage field and principal field on the effective active dielectric coefficient. The method makes it possible to calculate the eigenfrequencies of the resonators with considerable more accuracy than was previously possibly.

We thank Prof. Dr. H. Döring for the critical review of this work and many suggestions for improvement. The numerical calculations were done at the computer center of the Technical College, Aachen.

REFERENCES

1. Watkins, J. Circular Resonant Structures in Microstrip. Electron. Letters, Vol. 5, 1969, pp. 524-525.
2. Kirchhoff, G. Collected Transactions. Leipzig, 1882, pp. 101-113.
3. Zinke, O. Resistors, Condensers, Coils and their Materials. Springer-Verlag, Berlin, 1965, p. 82.
4. Wolff, I. Static Capacitors of Rectangular and Circular Microstrip Disc Condensers. AEU, Vol. 27, 1973, pp. 44-47.

5. Ollendorff, F. Fundamentals of High Frequency Technology. Springer-Verlag, Berlin, 1926, pp. 45-54.
6. Baier, W. Waves and Evanescent Fields in Rectangular Waveguides Filled with a Transversely Inhomogeneous Dielectric. Transact. Inst. Elect. Electron. Engrs. MTT-18, 1970, pp. 696-705.
7. Wolff, I. Measurement of Effective Dielectric Coefficients of Straight and Curved Waveguides on Coupled Microstrip Lines. Vol. 27, 1974, pp. 30-34.
8. Wheeler, H. A. Transmission-Line Properties of Parallel Strips Separated by a Dielectric Sheet. Transact. Inst. Elect. Electron. Engrs. MTT-13, 1965, pp. 172-185.
9. Schneider, M. V. Microstrip Lines for Microwave Integrated Circuits. Bell Syst. Tech. J. Vol. 48, 1969, pp. 1421-1444.

Translated for National Aeronautics and Space Administration under contract No. NASw 2483, by SCITRAN, P. O. Box 5456, Santa Barbara, California, 93108.